

Synthesis, Characterization, Cytotoxic and DNA Binding Studies of Diimine Platinum(II) and Palladium(II) Complexes of Short Hydrocarbon Chain Ethyldithiocarbamate Ligand

M. Islami-Moghaddam^a, H. Mansouri-Torshizi^{a,*}, A. Divsalar^b and A.A. Saboury^b

^aDepartment of Chemistry, University of Sistan & Baluchestan, Zahedan, Iran

^bInstitute of Biochemistry and Biophysics, University of Tehran, Tehran, Iran

(Received 9 May 2008, Accepted 13 August 2008)

Two novel Platinum(II) and Palladium(II) complexes of 2,2'-bipyridine (bpy) with ethyldithiocarbamate (Et-dtc) were synthesized. These complexes were characterized by spectroscopic methods such as ultraviolet-visible, infrared and ¹H NMR as well as conductivity measurements and chemical analysis. In these complexes, the dithiocarbamate ligand coordinates with Pt(II) or Pd(II) center as bidentate with two sulfur atoms. These water soluble complexes were tested for their *in vitro* anti-tumor activity against chronic myelogenous leukemia cell line, K562. They show Cc₅₀ values lower than those of cisplatin. The mode of binding of the complexes to calf thymus DNA, were investigated by circular dichroism, ultraviolet difference and fluorescence spectroscopy. These complexes can denature DNA at very low concentrations (~100 μM). Both complexes exhibit cooperative binding and presumably intercalate into DNA. Remarkably, most of the experimental results indicate that the tendency of the Pd(II) complex to interact with DNA and its anti-tumor activity against K562 is more than that of its Pt(II) analog.

Keywords: Cytotoxicity, Platinum(II) and Palladium(II) complexes, Ethyldithiocarbamate, DNA binding

INTRODUCTION

cis-Diamminedichloroplatinum(II) (cisplatin) is effective in the treatment of 70-90% of testicular tumors. Similarly, in combination with other drugs, it is effective against ovarian, small cell lung, bladder, brain and breast tumors [1]. However, it has several side-effects, and of particular importance is the renal damage which is correlated to Platinum binding and inactivation of renal thiol-containing enzymes [2,3]. A large number of analogs of cisplatin have been tested and it has been reported that many active complexes could react with DNA and inhibit its synthesis [4-8]. Other transition metal complexes with favorable anti-tumor activity are Gold,

Rhodium and Palladium complexes [2,3]. The development of Palladium anti-cancer drugs has not been promising and their design has mainly been based on the structural-activity relationship used for Platinum anti-cancer drugs as well as good models for the analogous Pt(II) complexes in solution. This is mainly because Palladium complexes are about 10⁵ times more reactive than their Pt(II) analogs leading to rapid hydrolysis of the leaving group/groups, thus the reactive species formed are unable to reach their pharmacological targets [9]. This problem may be solved by looking for Pd(II) compounds having chelating ligand which may not readily hydrolyze. A versatile class of such chelating ligands is dithiocarbamates. These compounds have the ability to stabilize transition metals in a wide range of oxidation states [10,11] and in health care for the management of alcoholism

*Corresponding author. E-mail: hmtorshizi@hamoon.usb.ac.ir

[12]. Dithiocarbamates have been applied to prevent arthrosclerosis [13]. They are also used as scavengers in waste-water treatment and floatation agents [14]; their antimicrobial activity and anti-inflammatory and metal transport in membranes have been reported [15,16].

Studies on sulfur-bonding chemoprotective agents have suggested that dithiocarbamates are the best rescue agents in an S-donor series of thiourea, thiosulfate and glutathione against cisplatin toxicity [17]. An example is diethyldithiocarbamate which inhibits the nephrotoxicity of cisplatin and has the remarkable property of reversing Platinum binding to the macromolecules responsible for host toxicity. However, it does not interfere with the tumoricidal Platinum-DNA interaction in the tumor cell [9]. It has been suggested that the protective action of diethyldithiocarbamate against the toxicity of cisplatin may be due to the formation of Platinum dithiocarbamate complex [18]. The antitumor activity of several dithiocarbamate complexes of the general formula $[M(S_2CNEt_2)(L)]NO_3$ ($M = Pd$ or Pt ; $L = 2,2'$ -bipyridine or 1,10-phenanthroline) against leukaemic cells has been established. Recently, a new class of Platinum(II) and Palladium(II) complexes containing dithiocarbamate ligands and various amines such as pyridine, n-propylamine, cyclobutylamine and ethylenediamine have been reported, and in most cases, their cytotoxic activity was greater than cisplatin [19]; moreover, they also showed no cross-resistance with cisplatin and very low *in vitro* and *in vivo* nephrotoxicity [20].

In this study, we selected two structurally related α -diiminealkyldithiocarbamate-ligated Platinum(II) and Palladium(II) complexes. These complexes have short non-polar hydrocarbon tails in their dithiocarbamate moieties which contribute to their water soluble nature whereas the lack of water solubility of some of the Platinum and Palladium complexes is the main reason for their limited bioavailability, and consequently low *in vivo* activity [21]. Moreover, both the compounds show higher cytotoxicity as compared to cisplatin and their probable target is DNA of the cells [4-8]. It is worth mentioning that only few contributions the the DNA binding studies of such dithiocarbamate complexes are available in literature [18,22]. Thus, the main purpose of the present work is to extend DNA-binding studies of Pt(II) and Pd(II) dithiocarbamate anti-tumor complexes. It may throw light on

the mechanisms of interaction of these agents with DNA which must be quite different from that of cisplatin, and detailed knowledge of the binding mode and interaction between nucleic acids with these species will be beneficial for medical science and pharmacokinetics. In these interaction studies, thermodynamic parameters, binding parameters and types of binding between metal complexes and DNA are also reported.

EXPERIMENTAL

Materials and General Methods

Palladium(II) chloride anhydrous was obtained from Fluka (Switzerland). Ethylamine and carbon disulfide were purchased from Aldrich (England). Potassium tetrachloroplatinate, 2,2'-bipyridine, highly polymerized calf thymus DNA sodium salt and Tris-HCl buffer were obtained from Merck (Germany). Other chemicals used were of analytical reagent or higher purity grade. Solvents used were of reagent grade and purified before use by the standard methods. $[Pt(bpy)Cl_2]$ and $[Pd(bpy)Cl_2]$ were prepared by the procedures described in the literature [23].

Conductivity measurements of the above Platinum and Palladium complexes were carried out on a Systronics conductivity bridge 305, using a conductivity cell of cell constant 1.0. Doubly distilled water was used as solvent. Electronic absorption spectra of the title metal complexes were measured on a J_{AS.CO} UV/VIS-7850 recording spectrophotometer. Infrared spectra of the metal complexes were recorded on a J_{AS.CO}-460 Plus FT-IR spectrophotometer in the range of 4000-400 cm^{-1} in KBr pellets. Microchemical analysis of carbon, hydrogen and nitrogen for the complexes were carried out on a Herause CHNO-RAPID elemental analyzer. ¹H NMR spectra were recorded on a Bruker DRX-500 Avance spectrometer at 500 MHz in DMSO-*d*₆ using tetramethylsilane as internal reference. Melting points were measured on a Unimelt capillary melting point apparatus and reported uncorrected.

Synthesis of Ligand and Metal Complexes

Synthesis of Et-dtcNa. This ligand was prepared by a modified literature method [24]: A solution of sodium hydroxide (4.00 g, 0.1 mol) in 30 ml doubly distilled water

was added to a stirred solution of ethylamine (8 ml of 70 wt.% solution in water, 0.10 mol) in acetone (10 ml). The reaction mixture was placed in an ice bath and an excess of carbon disulfide (10.0 ml) was added slowly with constant stirring. The resulting yellowish solution was stirred in a closed vessel at 0 °C for 2 h and at room temperature for 5 h. The solvent was removed on a rotary evaporator (40 °C) to complete dryness. The solid residue was suspended in 40 ml acetone, well-stirred and the white powder was filtered off and washed with 30 ml acetone and dried in a desiccator under vacuum. Recrystallization was carried out by stirring the crude product in 40 ml methanol at 25 °C and filtering out the small solid residue. Dichloromethane (40 ml) was then added to the final filtrate and allowed to stand undisturbed in refrigerator for 48 h. The desired product was collected by filtration as white powder and recrystallized once more, washed with dichloromethane and vacuum dried. Yield: 10.28 g (72%) with a melting point of 73 °C. Anal. Calcd. for $C_3H_6NS_2Na$ (143.11): C, 25.17; H, 4.20; N, 9.79. Found: C, 25.09; H, 4.21; N, 9.80%.

Synthesis of [Pt(bpy)(Et-dtc)]NO₃. [Pt(bpy)Cl₂] 0.422 g, 1 mmol was suspended in 120 ml acetone-water (3:1 v/v) mixture and 0.34 g, 2 mmol AgNO₃ was added to it with constant stirring. This reaction mixture was heated with stirring under dark for 6 h at 60 °C and then 15 h at room temperature (30 °C). The AgCl precipitate was filtered through Whatman 42 filter paper. To the clear yellow filtrate containing [Pt(bpy)(H₂O)₂](NO₃)₂, was slowly added a solution of 0.143 g, 1 mmol ethyldithiocarbamate sodium salt in 15 ml of acetone water mixture. Stirring continued at 45-50 °C for another 6 h and the volume of the solution was reduced to 30 ml at 40 °C. The volume of the mixture was then increased to 100 ml by doubly distilled water, stirred at 45-50 °C for 1-2 h and filtered. The volume of the filtrate was reduced to 5 ml and cooled. The product was collected as an orange precipitate, washed with 5 ml chilled water and then 10 ml acetone and dried at 40 °C. Yield: 0.352 g (66%) and decomposes at 235 °C. Anal. Calcd. for $C_{13}H_{14}N_4O_3S_2Pt$ (533): C, 29.27; H, 2.63; N, 10.51%. Found: C, 29.10; H, 2.71; N, 10.39%.

Synthesis of [Pd(bpy)(Et-dtc)]NO₃. 0.5 g (1.5 mmol) of [Pd(bpy)Cl₂] was well-suspended in 60 ml acetone-water (3:1 v/v) mixture and stirred vigorously for few hours. 0.51 g (3

mmol) of AgNO₃ was then added and the reaction mixture stirred for 2 h in dark under reflux at 45-50 °C. The AgCl precipitate was filtered through Whatman 42 filter paper. While the clear yellow filtrate containing [Pd(bpy)(H₂O)₂](NO₃)₂ was kept at 45 °C, 0.214 g (1.5 mmol) ethyldithiocarbamate sodium salt dissolved in 10 ml doubly distilled water was added dropwise. Stirring continued at 45 °C for another 2 h and filtered. The clear yellowish orange filtrate was concentrated to 8 ml at 30 °C. Diffusion of acetone into this filtrate for three days gave a brown precipitate. This precipitate was isolated by filtration, washed with 5 ml chilled water followed by 10 ml acetone and dried at 40 °C. Yield: 0.33 g (74%) and decomposes at 225.8-228.0 °C. Anal. Calcd. for $C_{13}H_{14}N_4O_3S_2Pd$ (444): C, 35.14; H, 3.15; N, 12.61%. Found: C, 35.03; H, 3.12; N, 12.67%.

Cytotoxic Studies

Cell culture. Chronic myelogenous leukemia cells were grown in RPMI medium supplemented with L-glutamine (2 mM), Streptomycin and penicillin (5 µg ml⁻¹) and 10% heat-inactivated fetal calf serum, at 37 °C under a 5% CO₂/95% air atmosphere.

Cell proliferation assay. The growth inhibitory effect of Pd(II) and Pt(II) complexes towards the cells was measured by means of MTT assay. The cleavage and conversion of the soluble yellowish MTT to the insoluble purple formazan by active mitochondrial dehydrogenase of living cells was used to develop an assay system alternative to other assays for measurement of cell viability. Harvested cells were seeded into 96-well plate (1 × 10⁴ cell/ml) with varying concentrations of the sterilized drugs (0-250 µM) and incubated for 24 h. Four hours to the end of incubations, 25 µl of MTT solution (5 mg ml⁻¹ in PBS) was added to each well containing fresh and cultured medium [4].

At the end, the insoluble formazan produced was dissolved in solution containing 10% SDS and 50% DMF (Left for 2 h at 37 °C in dark conditions) and optical density (OD) was read against reagent blank with multi well scanning spectrophotometer (ELISA reader, Model Expert 96, Asys Hitchech, Austria) at a wavelength of 570 nm. Absorbance was a function of concentration of converted dye. The OD value of study groups was divided by the OD value of untreated control and presented as percentage of control (as

100%).

Statistical analysis. Results were analyzed for statistical significance using two-tailed independent samples t-test. Changes were considered significant at $p < 0.05$.

Binding Studies

The difference ultraviolet visible absorption were used to determine the binding parameters of the metal complexes to DNA [22,25]. The stock solutions of Pt(II) and Pd(II) complexes (1.4 mM) were made in the above mentioned Tris-HCl buffer of pH 7.0 medium containing 10 mM sodium chloride by gentle stirring and heating at 35 °C, while that of DNA (4 mg ml⁻¹) at 4 °C until homogenous. The metal complex solutions, with and without DNA were incubated at 27 °C and 37 °C. Then, the spectrophotometric readings at λ_{max} (nm) of complexes where DNA has no absorption were measured. Using trial and error method, the incubation time for solutions of DNA-metal complexes at 27 °C and 37 °C was found to be 6 h and 30 min, respectively. No further changes were observed in the absorbance reading after longer incubation. The concentration of DNA was found out based on determination of phosphate (P). Millimolar extinction coefficient of native DNA solution at E₂₅₈ (ϵ_{258}) based on DNA P, was 6.6×10^3 [26]. In the binding studies of the above complexes with DNA five main experiments were carried out:

(i) A fixed amount of each metal complex was titrated with increasing concentration of DNA at 27 °C and 37 °C, separately. In this experiment, change in absorbance, ΔA , was calculated by subtracting the absorbance reading of mixed solutions of each metal complex with various concentrations of DNA, from absorbance reading of free metal complex. The maximum ΔA (ΔA_{max}) of the metal complex totally bound to DNA was determined by intrapolation of a plot of reciprocal of ΔA s against the reciprocal of [DNA] obtained from each DNA concentration (*i.e.*, intercept on ordinate). This ΔA_{max} was used to calculate the concentration of bound metal complex with DNA in the next experiment.

(ii) A fixed amount of DNA was titrated with varying concentration of each metal complex. Here, also the ΔA s for each concentration of metal complex were calculated as in experiment (i) at λ_{max} (nm) of each metal complex. Now, the concentration of metal complex bound to DNA, $[L]_b$, was obtained using the Eq. (1) [27].

$$[L]_b = \Delta A [L]_t / \Delta A_{\text{max}} \quad (1)$$

where ΔA_{max} and ΔA were determined from experiment (i) and (ii), respectively and $[L]_t$ is the maximum concentration of metal complex added to saturate all the binding sites of DNA. The concentration of the free metal complex, $[L]_f$, can be calculated from Eq. (2) and \bar{v} , the ratio of the concentration of bound metal complex to the total DNA concentration from Eq. (3).

$$[L]_f = [L]_t - [L]_b \quad (2)$$

$$\bar{v} = [L]_b / [DNA]_t \quad (3)$$

The Scatchard plots were obtained separately at 27 °C and 37 °C by plotting $\bar{v} / [L]_f$ vs. \bar{v} . From the nature of the plot, the type of cooperativity can be verified (concave downward curve indicates cooperative, concave upward anti-cooperative and straight line non-cooperative). Also, the binding isotherm was constructed by plotting \bar{v} vs. $\text{Ln}[L]_f$ (sigmoid curves, are characteristic of positive cooperative binding, hyperbolic nature of the curve shows non-cooperative) [28].

On substituting the values of \bar{v} and $[L]_f$ in Hill equation (see Eq. (4)), we get a series of equations with unknown parameters n , K and g .

$$\bar{v} = \frac{g(K[L]_f)^n}{1 + (K[L]_f)^n} \quad (4)$$

where n is the Hill coefficient ($n = 1$ indicates non-cooperative, $n > 1$ is cooperative and $n < 1$ shows anti-cooperative binding of macromolecule with metal complex), g is the number of binding sites per thousand nucleotides for DNA and K is the apparent binding constant [29,30]. Using Eureka software [31] (where fitting is based on nonlinear least-square), these series of equations were solved and the theoretical values of n , K and g were deduced. The Hill plot can be obtained by plotting $\text{Ln}(\bar{v}/g - \bar{v})$ vs. $\text{Ln}[L]_f$ at both 27 °C and 37 °C. The sigmoidal nature of this plot shows that the metal complex-macromolecule interaction is cooperative.

In addition, the Wyman binding potential (Π) can be calculated from the area under the binding isotherm according to the Eq. (5) [32]. Also, the Jons binding potential (Π) can be

calculated from the Eq. (6) [32].

$$\Pi = RT \int v d \ln [L]_f \quad (5)$$

$$\Pi = RT L n [1 + K_{app} [L]_f^v] \quad (6)$$

where R is gas constant and T is temperature in K. $[L]_f$ and K_{app} are concentration of free ligand and apparent binding constant for each particular v , respectively. From Eqs. (5) and (6), we get the Eq. (7):

$$\int v d \ln [L]_f = L n [1 + K_{app} [L]_f^v] \quad (7)$$

Now, the values of K_{app} can be calculated from Eq. (7) at the two temperatures 27 °C and 37 °C for each particular v . Using the values of K_{app} , we can determine the corresponding values of molar Gibbs free energy of binding (ΔG_b°) from Eq. (8) and molar enthalpy of binding (ΔH_b°) from Eq. (9). Also the molar entropy of binding (ΔS_b°) in the interaction of metal complex with macromolecule can be found from Eq. (10) [33].

$$\Delta G_b^\circ = -RT \ln K_{app} \quad (8)$$

$$L n \frac{K_{app, T_1}}{K_{app, T_2}} = -\frac{\Delta H_b^\circ}{R} \left(\frac{1}{T_2} - \frac{1}{T_1} \right) \quad (9)$$

$$\Delta G_b^\circ = \Delta H_b^\circ - T \Delta S_b^\circ \quad (10)$$

Finally, the values of ΔH_b° is plotted vs. the values of $[L]_f$ and \bar{v} in a single plot. This plot is a sort of standard from which ΔH_b° in each $[L]_f$ for each \bar{v} can be calculated.

(iii) The above mentioned metal complexes can denature DNA. The task of this experiment was finding thermodynamic parameters of DNA. It was done by looking at the changes in the UV absorption spectrum of DNA solution at 258 nm upon addition of Platinum(II) and Palladium(II) complexes. In this experiment, the sample cell was filled with 1.8 ml DNA (0.04 mg ml⁻¹ or 0.08 mM). In these concentrations, the absorption of DNA is around 0.6. However, reference cell is filled with 1.8 ml Tris-HCl buffer only. Both cells were set separately at constant temperature of 27 °C or 37 °C and then 25 μ l solution of metal complex (1.4 mM) was added to each cell. After 3

min, the absorption was recorded at 258 nm for DNA and at 640 nm to eliminate the interference of turbidity. Addition of metal complex to both cells was continued until no further changes in the absorption readings were observed. These absorption readings of DNA solutions were plotted separately versus different concentrations of metal complexes. From these plots, the concentration of each metal complex at midpoint of transition, $[L]_{1/2}$, could be deduced for the two temperatures 27 °C and 37 °C, separately. Using these plots, we can calculate the ratio of concentration of metal complex to the concentration of DNA in the transition region because the experiment (i) and (ii) should be carried out at these regions. Now, thermodynamic parameters in the process of denaturation can be determined using the above plots and Pace method [34]. In this method, Pace had assumed two-state mechanism, nature and denature, and then calculated unfolding free energy of DNA *i.e.* (ΔG°) by using Eqs. (11) and (12):

$$K = \frac{A_N - A_{obs}}{A_{obs} - A_D} \quad (11)$$

$$\Delta G^\circ = -RT \ln K \quad (12)$$

where A_{obs} is absorbance readings in transition region, A_N and A_D are absorbance readings of nature and denatured conformation of DNA, respectively. A straight line is obtained when ΔG° 's are plotted versus concentrations of metal complex in transition region at 27 °C and 37 °C, separately. The equation for these lines can be written as follows [26,35]:

$$\Delta G^\circ = \Delta G^\circ_{(H_2O)} - m[\text{complex}] \quad (13)$$

where $\Delta G^\circ_{(H_2O)}$ is conformational stability of DNA in the absence of metal complex and m is a measure of the metal complex ability to denature DNA. Here, the molar enthalpy of DNA denaturation by the metal complex, $\Delta H^\circ_{\text{denaturation}}$ or $\Delta H^\circ_{\text{conformation}}$, in the range of the two temperatures can be calculated using Gibbs-Helmholtz equation as follows [36]:

$$\Delta H^\circ = \frac{\frac{\Delta G^\circ(T_1)}{T_1} - \frac{\Delta G^\circ(T_2)}{T_2}}{\frac{1}{T_1} - \frac{1}{T_2}} \quad (14)$$

where $\Delta G^\circ_{(T_1)}$ and $\Delta G^\circ_{(T_2)}$ are the Gibbs free energies of DNA denaturation at $T_1 = 300$ K and $T_2 = 310$ K, respectively. In addition, the molar enthalpy of DNA denaturation in the absence of metal complex, $\Delta H^\circ_{(H_2O)}$, was determined by intrapolation of a plot of ΔH° against the concentration of metal complex. Also, the molar entropy of DNA denaturation in the absence of metal complex, $\Delta S^\circ_{(H_2O)}$, was calculated using Eq. (15).

$$\Delta G^\circ_{(H_2O)} = \Delta H^\circ_{(H_2O)} - T\Delta S^\circ_{(H_2O)} \quad (15)$$

Higher values of $\Delta G^\circ_{(H_2O)}$ and $\Delta H^\circ_{(H_2O)}$ indicate a higher stability of the macromolecule. However, higher values of $\Delta S^\circ_{(H_2O)}$ show that the macromolecule is in a state of denature or disorder and lower values indicate nature or order.

Experiments (iv) and (v) were carried out according to our previous report [37].

Fluorescence Studies

Fluorescence intensity measurements were carried out on a Hitachi spectrofluorimeter model MPF-4. The maximum quantum yield for ethidium bromide was achieved at 471 nm, so we selected this wavelength as excitation radiation for all samples at different temperatures (27 °C and 37 °C) in the range of 540-700 nm. Measurements were done by applying a 1-cm path length fluorescence cuvette. At first, 60 μ M DNA was added to 2 μ M aqueous ethidium bromide solution. Here the fluorescence of ethidium bromide is enhanced about 50-fold on its intercalation between base pairs of DNA [38]. Since the fluorescence intensity of DNA-ethidium complex can be altered on binding of metal complex to DNA-ethidium [39], the effect of [Pt(bpy)(Et-dtc)]NO₃ and [Pd(bpy)(Et-dtc)]NO₃ on the fluorescence intensity of DNA-ethidium was studied. Thus titration of DNA-ethidium with Pd(II) or Pt(II) complex covering a range of [complex]/[DNA] ratio in transition region (found from denaturation experiment of DNA by these metal complexes), were performed with increasing concentration of each metal complex (0.05, 0.1 and 0.15 mM). The fluorescence intensities of the Pd(II) and Pt(II) complexes at the highest denaturant concentration at 471 nm excitation wavelength were checked and it was found that the emission intensities of these compounds were very small and negligible.

Circular Dichroism Studies

Circular dichroism (CD) spectra were recorded on an Aviv Spectropolarimeter model 215. Changes in the structures of DNA were monitored in the region (200-320 nm) using 1 cm path length cells [38,39]. The DNA concentration in the experiments was 120 μ M. Induced CD spectra resulting from the interaction of the Pd(II) or Pt(II) complex with DNA were obtained by subtracting the CD spectrum of the native DNA and mixture of DNA-Pd(II) or Pt(II) complex from the CD spectrum of the buffer and spectrum of buffer-Pd(II) and Pt(II) complex solutions at the two temperatures 27 °C and 37 °C.

RESULTS AND DISCUSSION

Two complexes of the formula [M(bpy)(Et-dtc)]NO₃ (where M is Pt(II) or Pd(II), Et-dtc is ethyldithiocarbamate) were synthesized by interaction of an appropriate [Pt(bpy)(H₂O)₂](NO₃)₂ or [Pd(bpy)(H₂O)₂](NO₃)₂ [7] with sodium ethyldithiocarbamate in molar ratio of 1:1. The molar conductance values of these complexes in water are given in Table 1. These values are in the range of 118 to 131 cm² ohm⁻¹ mol⁻¹ suggesting that the complexes are 1:1 electrolytes [40].

The maximal absorption bands in electronic absorption spectra of the above Platinum(II) and Palladium(II) complexes in distilled water with their extinction coefficients [41] are given in Table 1 and assigned as follows. Band I in the Platinum complex is assigned to metal to ligand charge transfer (MLCT) because band I is blue shifted by 10 to 15 nm on going from acetone to water. In this complex band I may be due to charge transfer from Platinum to π^* of 2,2'-bipyridine ligand. However, band I may as well be due to the charge transfer from Platinum to π^* of dithiocarbamate [42]. However, this type of charge transfer transition is not observed in 2,2'-bipyridine and 1,10-phenanthroline analogous complexes reported earlier [18] because it may be hidden in much stronger charge transfer transition from Platinum to π^* of 2,2'-bipyridine or 1,10-phenanthroline ligands. Bands II, III, IV and V in Platinum complex may be due to first, second, and higher internal $\pi \rightarrow \pi^*$ transitions of 2,2'-bipyridine ligand [18]. Bands III, IV and V in the Platinum complex have also overlapping components of $\pi \rightarrow \pi^*$ transitions of dithiocarbamate ligand. The above electronic absorption data suggest that this complex has square planar configuration [43].

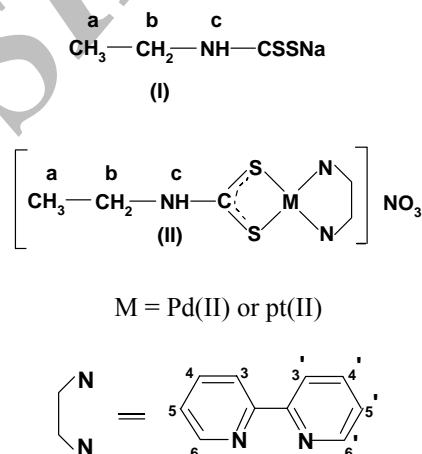
Table 1. Electronic Absorption Bands and Molar Conductance Values of [Pt(bpy)(Et-dtc)]NO₃ and [Pd(bpy)(Et-dtc)]NO₃ Complexes in Water

Compound	Band maxima in nm					Molar conductance of 1×10^{-4} solution ($\text{cm}^2 \text{ohm}^{-1} \text{mol}^{-1}$)
	Band I	Band II	Band III	Band IV	Band V	
[Pt(bpy)(Et-dtc)]NO ₃	363(3.27)	321(6.85) ^a	310(6.40)	283(1.16)	207(2.40)	105
[Pd(bpy)(Et-dtc)]NO ₃	-	313(1.23)	305(1.29)	247(3.89)	203(3.56)	109

^aExtinction coefficients in $1 \text{ mol}^{-1} \text{ cm}^{-1} \times 10^{-4}$ are given in parenthesis.

In Palladium complex, bands II and III are blue shifted by 13 and 14 nm, respectively on going from less polar chloroform to more polar dimethylsulfoxide. Therefore, these bands can tentatively be assigned to charge transfer from Palladium to 2,2'-bipyridine ligand. Bands IV and V are assigned to first and higher internal $\pi \rightarrow \pi^*$ transition of 2,2'-bipyridine. Also, bands III, IV and V have overlapping components of $\pi \rightarrow \pi^*$ transitions of dithiocarbamate ligand.

The IR spectra of the above ligands and complexes are recorded in the range 4000-400 cm^{-1} as KBr pellets. Two important bands are of interest. The Et-dtcNa ligand shows a strong absorption at 1510 cm^{-1} . This band, which is assigned to the N-CSS stretching mode [44], appears at 1522 and 1561 cm^{-1} in the IR spectra of [Pt(bpy)(Et-dtc)]NO₃ and [Pd(bpy)(Et-dtc)]NO₃, respectively. These data suggest that the N-CSS bond order is in between a single bond ($\nu = 1250-1350 \text{ cm}^{-1}$) and a double bond ($\nu = 1640-1690 \text{ cm}^{-1}$) [45]. As is evident from the IR spectral data of the free dithiocarbamate ligand and the corresponding complexes, the $\nu(\text{N-CSS})$ mode has shifted to higher frequencies upon coordination. This indicates that the nitrogen-carbon double bond character has increased due to the electron delocalization towards the Platinum or Palladium centers. Thus, the above ethyldithiocarbamate ligand coordinates with Pt(II) or Pd(II) through sulfur atoms. The second interesting feature in the IR spectra of the Et-dtc ligand and its metal complexes is the presence of a single strong band at 965 cm^{-1} for Et-dtcNa and at 1035, 1036 cm^{-1} for [Pt(bpy)(Et-dtc)]NO₃ and [Pd(bpy)(Et-dtc)]NO₃, respectively. This band is attributed to $\nu(\text{SCS})$ mode which is indicative of symmetrical bonding of the dithionate ligand, acting in a bidentate mode in our complexes (Fig. 1).


Fig. 1. Proposed structures and nmr numbering schemes of (I) Et-dtcNa, (II) [Pt(bpy)(Et-dtc)]NO₃ or [Pd(bpy)(Et-dtc)]NO₃

Otherwise a doublet would be expected in the $1000 \pm 70 \text{ cm}^{-1}$ region which indicates an asymmetrically bonded ligand or a monodentate bound ligand [2].

The ¹H NMR spectral data of ethyldithiocarbamate ligand and its corresponding 2,2'-bipyridine Platinum(II) and Palladium(II) complexes in DMSO-d₆ are summarized in Table 2. The proposed structure and nmr numbering scheme are given in Fig. 1. In the ¹H NMR spectrum of Et-dtcNa, the triplet observed at δ 1.25, a multiplet at δ 3.69 and a broad singlet at δ 10.18 are assigned to H-a, H-b and H-c protons, respectively (see Fig. 1 and Table 2). The signal due to the H-c protons in the spectra of [Pt(bpy)(Et-dtc)]NO₃ and [Pd(bpy)(Et-dtc)]NO₃ complexes appears at δ 11.59 and δ

Table 2. ¹H NMR Spectral Data of Et-NH-CSSNa Ligand and [M(bpy)(Et-NH-CSS)]NO₃ Complexes in Deuterated DMSO

Compound	Dithiocarbamate protons			2,2'-Bipyridine protons		
	δH-a	δH-b	δH-c	δH-6,6'	δH-4,4' and δH-3,3'	δH-5,5'
Et-dtcNa	1.25 ^a (t) ^β	3.69(m)	10.18(sb)	-	-	-
[Pt(bpy)(Et-dtc)]NO ₃	1.24(t)	3.48(m)	11.59(sb)	8.66(m)	8.41(m)	7.71(m)
[Pd(bpy)(Et-dtc)]NO ₃	1.25(t)	3.58(m)	11.68(sb)	8.70(m)	8.36(m)	7.77(m)

^aChemical shift in ppm. ^βs, d, t, q, m and sb are singlet, doublet, triplet, quartet, multiplet and singlet broad, respectively.

11.68, respectively. The downfield shift of 1.41 ppm in [Pt(bpy)(Et-dtc)]NO₃ and 1.5 ppm in [Pd(bpy)(Et-dtc)]NO₃ as compared to the free ligand indicates the bidentate coordination of Et-dtcNa ligand to Pt(II) and Pd(II) and is consistent with the IR spectral data (*vide supra*).

The coordination of the dithiocarbamate ligand with Platinum or Palladium invariably produces a downfield shift in the position of its proton signals relative to those of the free dithiocarbamate ligand. The extent of this downfield shift decreases regularly with distance from the coordination site [46]. This is due to the electron donation by -CSS⁻ group to Palladium or Platinum. However, the signals corresponding to the H-6,6' (9.52 ppm) and H-5,5' (7.85 ppm) protons of the 2,2'-bipyridine moiety in [Pt(bpy)Cl₂] are invariably shifted upfield in the dithiocarbamate complexes (see Table 2) [18]. This may be explained in terms of back donation of electron density from Platinum or Palladium to 2,2'-bipyridine ligand as well as stronger binding of dithiocarbamate to Pt(II) or Pd(II) relative to the chloride anion in [Pt(bpy)Cl₂] or [Pd(bpy)Cl₂]. The protons of 2,2'-bipyridine in [Pt(bpy)(Et-dtc)]NO₃ appear as three multiplets centered at 8.66, 8.41 and 7.71 ppm which are assigned to H-6,6', H-4,4' H-3,3' and H-5,5' protons, respectively. Similar assignments were set for protons of 2,2'-bipyridine in the analogous complex [Pd(bpy)(Et-dtc)]NO₃. Thus, based on the spectroscopic data, the structures as shown in Fig. 1(II), were assigned to these two complexes which are also in accord with the observed molar conductance value of 105 and 109 cm² ohm⁻¹ mol⁻¹ for [Pt(bpy)(Et-dtc)]NO₃ and [Pd(bpy)(Et-dtc)]NO₃, respectively, as 1:1 electrolytes. Further support for the proposed structures come from the ratio of the integrated areas under the peaks of 2,2'-bipyridine and dithiocarbamate protons being 8:6 for

[Pt(bpy)(Et-dtc)]NO₃ and [Pd(bpy)(Et-dtc)]NO₃ complexes. Finally, no changes were observed in the ¹H NMR spectra of the above complexes dissolved in DMSO-d₆ and recorded after 24 h suggesting no dissociation of dithiocarbamate anions.

Cytotoxicity Measurement of the Pd(II) and Pt(II) Complexes

The *in vitro* anti-tumor properties of the synthesized complexes were studied by testing them on human tumor cell line K562 [4]. In this study, various concentrations of Pd(II) and Pt(II) complexes ranging from 0 to 250 μM of stock solutions were used to a culture of the tumor cell lines for 24 h (Fig. 2). The 50% cytotoxic concentration (C_{c50}) of each compound was determined 55 μM and 89 μM for Pd(II) and Pt(II) complexes, respectively (see Fig. 2).

As shown in Fig. 2, cell growing after 24 h was significantly reduced in the presence of various concentrations of the two compounds. Based on this figure it is also clear that the Pd(II) and Pt(II) complexes produced a dose response suppression on growing of K562 leukemia cell lines. The presence of Pd moiety in the structure of Pd(II) complex noticeably decreases its C_{c50} value (55 μM) which is considerably lower than the C_{c50} value of the Pt(II) complex (89 μM). Furthermore, C_{c50} value of cisplatin under the same experimental conditions was determined. This value (154 μM) is much higher as compared to the C_{c50} values of the above two complexes. However, the C_{c50} values of these complexes are slightly higher than those of our analogous Palladium(II) dithiocarbamate complexes reported earlier [4].

DNA Binding Studies

The values of ΔA_{max}, change in the absorbance when all

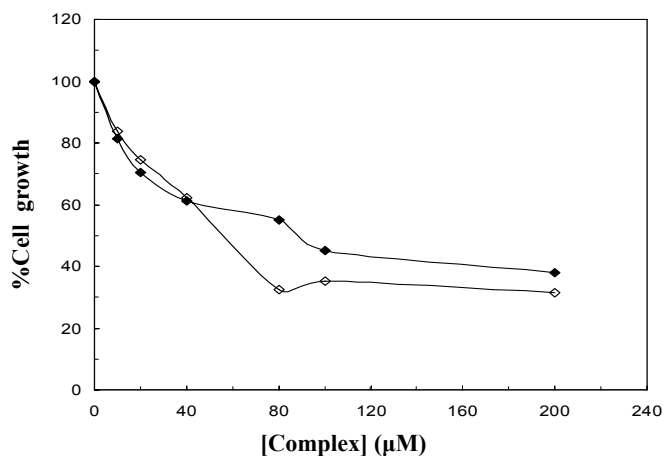


Fig. 2. The growth suppression activity of the Pd(II)-complex (\diamond) and Pt(II) complex (\blacklozenge) on K562 cell line was assessed using MTT assay as described in material and methods. The tumor cells were incubated with varying concentrations of the complexes for 24 h.

binding sites on DNA were occupied by metal complex, are given in Table 3 and Fig. 3(A) and 3(B). These values were used to calculate the concentration of metal complex bound to DNA, $[L]_b$, and the concentration of free metal complex, $[L]_f$ and $\bar{\nu}$, the ratio of the concentration of bound metal complex to total [DNA]. Using these data the Scatchard plots were constructed for the interaction of each metal complex at two temperatures of 27 °C and 37 °C. The Scatchard plots are shown in Fig. 4(A) and 4(B) for $[\text{Pt}(\text{bpy})(\text{Et-dtc})]\text{NO}_3$ and $[\text{Pd}(\text{bpy})(\text{Et-dtc})]\text{NO}_3$, respectively. These plots are curvilinear concave downwards, suggesting cooperative binding [28]. To

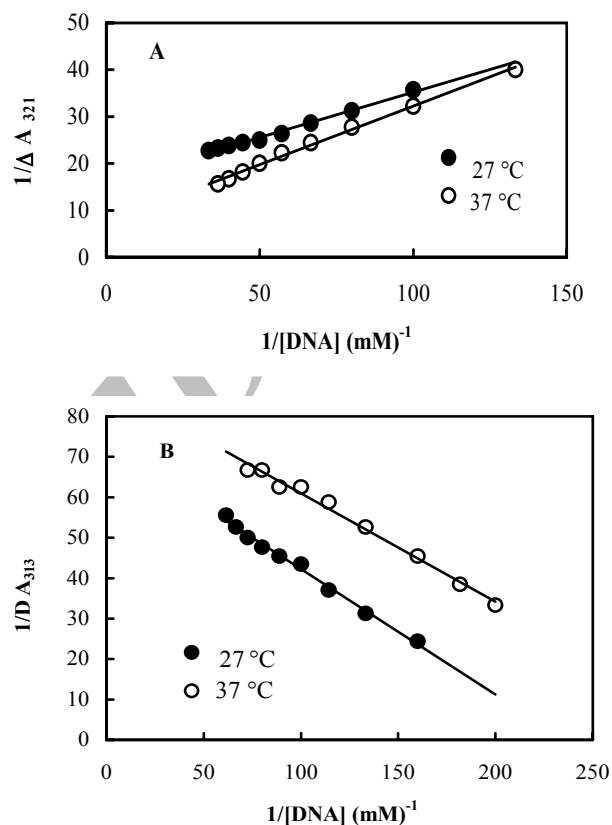


Fig. 3. The changes in the absorbance of fixed amount of each metal complex in the interaction with varying amount of DNA at 27 °C and 37 °C. The linear plot of the reciprocal of ΔA vs. the reciprocal of [DNA] for (A) $[\text{Pt}(\text{bpy})(\text{Et-dtc})]\text{NO}_3$ and (B) for $[\text{Pd}(\text{bpy})(\text{Et-dtc})]\text{NO}_3$.

Table 3. Values of ΔA_{max} and Binding Parameters in the Hill Equation for Interaction Between Pt(II) or Pd(II) Complexes and DNA in 10 mM Tris-HCl Buffer and pH 7.0

	Temperature	ΔA_{max}	g	$K \text{ (M)}^{-1}$	n	Error ^a
$[\text{Pt}(\text{bpy})(\text{Et-dtc})]\text{NO}_3$	27 °C	0.630	9	0.028	2.03	0.006
	37 °C	0.138	9	0.025	2.49	0.004
$[\text{Pd}(\text{bpy})(\text{Et-dtc})]\text{NO}_3$	27 °C	0.014	9	0.180	4.77	0.03
	37 °C	0.011	9	0.270	4.79	0.06

ΔA_{max} = change in the absorbance when all the binding sites on DNA were occupied by metal complex. g = the number of binding sites per 1000 nucleotides. K = the apparent binding constant. n = the Hill coefficient (as a criterion of cooperativity). ^a maximum error between theoretical and experimental values of $\bar{\nu}$.

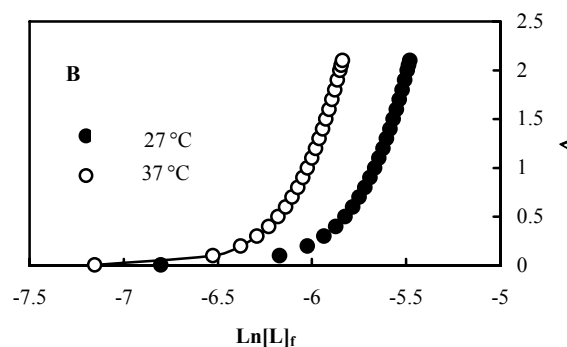
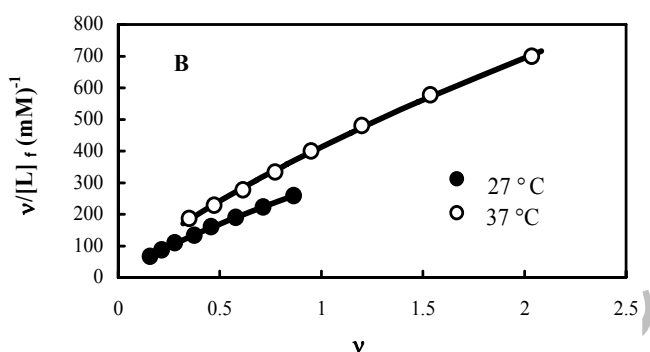
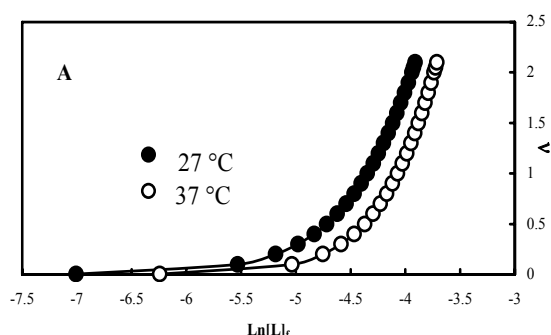
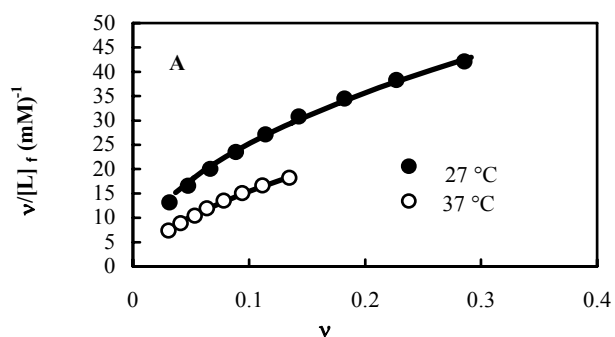


Fig. 4. Scatchard plots for binding of (A) $[\text{Pt}(\text{bpy})(\text{Et-dtc})]\text{NO}_3$ and (B) $[\text{Pd}(\text{bpy})(\text{Et-dtc})]\text{NO}_3$ (0.05-0.17 ml of 0.1 mM stock) to DNA (0.05 ml of 0.1 mM stock).

Fig. 5. Binding isotherm plots for (A) $[\text{Pt}(\text{bpy})(\text{Et-dtc})]\text{NO}_3$ and (B) $[\text{Pd}(\text{bpy})(\text{Et-dtc})]\text{NO}_3$ in the interaction with DNA.

obtain the binding parameters, the above experimental data ($[\text{L}]_f$ and \bar{v}) were substituted in Hill equation (Eq. (4)) to get a series of equation with unknown parameters n , K and g . Using Eureka software, the theoretical values of these parameters could be deduced. The results are tabulated in Table 3 which are comparable with those of 2,2'-bipyridine-Platinum and -Palladium complexes of dithiocarbamate as reported earlier [18]. The maximum error between experimental (Eq. (3)) and theoretical (Eq. (4)) values of \bar{v} are also shown in Table 3 which are quite low. The K , apparent binding constant in the interaction of $[\text{Pd}(\text{bpy})(\text{Et-dtc})]\text{NO}_3$ with DNA is higher than that of $[\text{Pt}(\text{bpy})(\text{Et-dtc})]\text{NO}_3$ with DNA (see Table 3). This indicates that the interaction affinity of Pd(II) complex to DNA is more than that of Pt(II) complex. This may be due to

the fact that Palladium complexes are about 10^5 times more labile than their Platinum analogs [9]. In addition, the data in Table 3 show that the values of n , the Hill coefficient (as a criterion of cooperativity) for Palladium complex are higher than those of Platinum analogs which is reflective of higher cooperativity of Pd(II) as compared with Pt(II) complex. The same observations can be made in the results of cytotoxic studies of these two compounds. Similar results were obtained for $[\text{Pd}(\text{bpy})(\text{ddtc})]\text{NO}_3 \cdot \text{H}_2\text{O}$ [18], though its Pt(II) analog is highly cooperative.

Having in mind the experimental (dots) and theoretical (lines) values of \bar{v} in the Scatchard plots and superimposability of them on each other, these values of \bar{v} were plotted vs. the values of $\text{Ln}[\text{L}]_f$. The results are sigmoidal curves and are shown in Fig. 5(A) and 5(B) at 27 °C and 37 °C. These plots

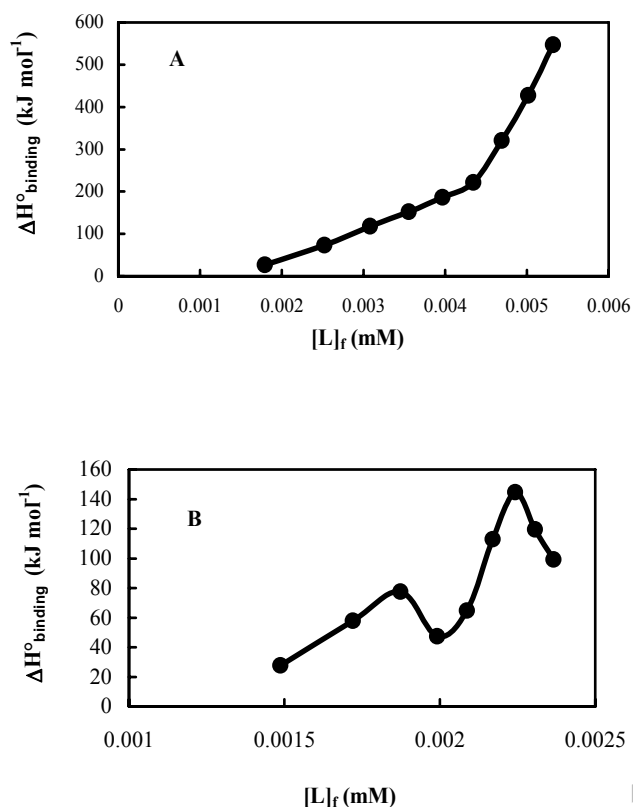


Fig. 6. Molar enthalpies of binding in the interaction between DNA and (A) $[\text{Pt}(\text{bpy})(\text{Et-dtc})]\text{NO}_3$ and (B) $[\text{Pd}(\text{bpy})(\text{Et-dtc})]\text{NO}_3$ vs. free concentrations of complexes at pH 7.0 and 27 °C.

indicate positive cooperative binding at both temperatures for both complexes. By detecting the area under the above plots of binding isotherms and using equations 5 to 9, we can calculate the K_{app} and ΔG_b° at 27 °C and 37 °C for each particular v and also ΔH_b° . Plots of the values of ΔH_b° vs. the values of $[\text{L}]_f$ are shown in Fig. 6(A) and 6(B) for $[\text{Pt}(\text{bpy})(\text{Et-dtc})]\text{NO}_3$ and $[\text{Pd}(\text{bpy})(\text{Et-dtc})]\text{NO}_3$ respectively at 27 °C. Deflections are observed in both plots. These deflections indicate that at particular $[\text{L}]_f$, there is a sudden change in enthalpy of binding which may be due to binding of metal complex to macromolecule or macromolecule denaturation.

The above Platinum(II) and Palladium(II) complexes can denature DNA. The profiles of denaturation of DNA by $[\text{Pt}(\text{bpy})(\text{Et-dtc})]\text{NO}_3$ and $[\text{Pd}(\text{bpy})(\text{Et-dtc})]\text{NO}_3$ are shown in

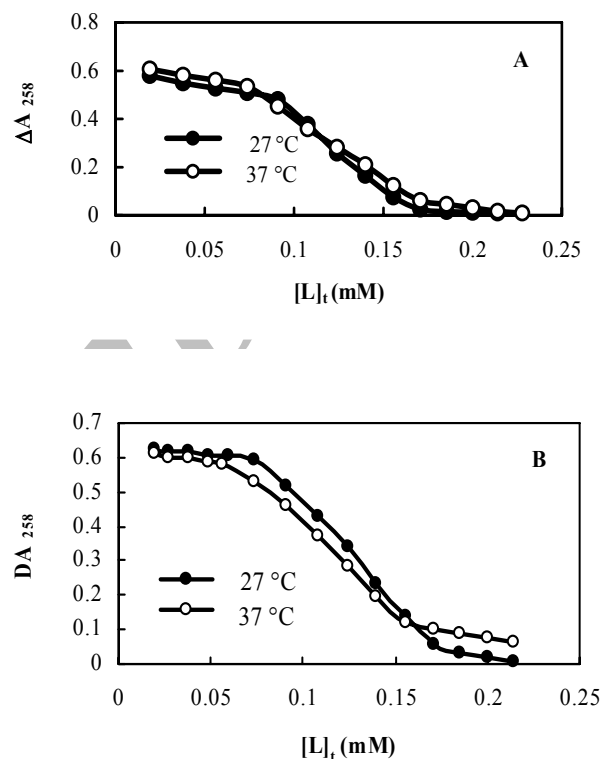


Fig. 7. The changes of absorbance of DNA (0.08 mM) at $\lambda_{\text{max}} = 258$ nm due to increasing the total concentration of (A) $[\text{Pt}(\text{bpy})(\text{Et-dtc})]\text{NO}_3$ and (B) $[\text{Pd}(\text{bpy})(\text{Et-dtc})]\text{NO}_3$, $[\text{L}]_t$, at constant temperature of 27 °C and 37 °C.

Fig. 7(A) and 7(B), respectively at two temperatures of 27 °C and 37 °C. The concentration of metal complexes in the midpoint of transition, $[\text{L}]_{1/2}$, for Pt(II) complex at 27 °C is 0.13 and at 37 °C is 0.122 mM and for Pd(II) complex at 27 °C is 0.121 and at 37 °C is 0.105 mM. The improving effect of the temperature, leading to the decrease in $[\text{L}]_{1/2}$ from 0.13 to 0.122 for Pt(II) system and from 0.121 to 0.105 for Pd(II) system, indicates that the increase in the temperature lowers the stability of the DNA against denaturation caused by these complexes. The important observation of this work is the low values of $[\text{L}]_{1/2}$ for these complexes [39,47-48] *i.e.* both complexes can denature DNA at very low concentrations. Thus, if these complexes are used as antitumor agents, low doses would be needed which would imply less side-effects.

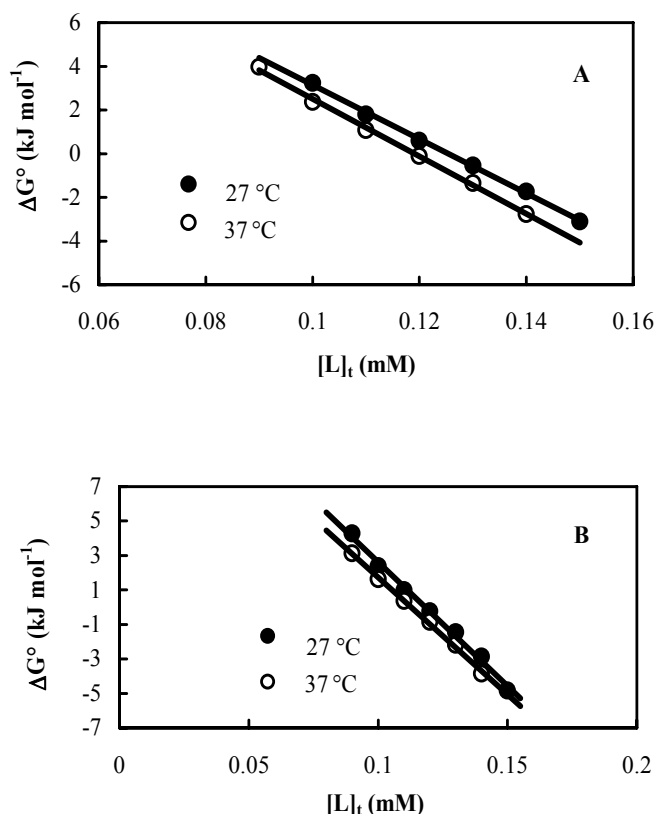


Fig. 8. The molar Gibbs free energies of unfolding (ΔG° vs. $[L]_i$) of DNA in the presence of (A) $[\text{Pt}(\text{bpy})(\text{Et-dtc})]\text{NO}_3$ and (B) $[\text{Pd}(\text{bpy})(\text{Et-dtc})]\text{NO}_3$.

Below some thermodynamic parameters found in the process of DNA denaturation are reported. Using the DNA denaturation plots given in Fig. 7 and Pace method [9], the values of K , unfolding equilibrium constant (Eq. (11)) and ΔG° , unfolding free energy (Eq. (12)) of DNA at two temperatures of 27 °C and 37 °C in the presence of $[\text{Pt}(\text{bpy})(\text{Et-dtc})]\text{NO}_3$ and $[\text{Pd}(\text{bpy})(\text{Et-dtc})]\text{NO}_3$ are calculated. A straight line is obtained when the values of ΔG° are plotted versus the concentrations of each metal complex in the transition region at 27 °C and 37 °C (Eq. (13)). These plots are shown in Fig. 8(A) and 8(B) for Pt(II) and Pd(II) systems, respectively. The m , slope of these plots (a measure of the metal complex ability to denature DNA) and the intercept on ordinate, $\Delta G^\circ_{(H_2O)}$, (conformational stability of DNA in the absence of metal complex) are summarized in Table 4. The values of m for Pd(II) complex are higher than those of Pt(II) complex which indicates the higher ability of Pd(II) to denature DNA. These m values are similar to Pd(II) complex as well as surfactant reported earlier [8]. As we know, the higher the value of ΔG° , the larger the conformational stability of DNA. However, the values of ΔG° (see Table 4) are decreased by increasing the temperature for both complexes. This is as expected because in general, most of the macromolecules are less stable at higher temperature. The same trend has been observed in the denaturation of calf thymus DNA with other denaturing agents [48].

Table 4. Thermodynamic Parameters of DNA Denaturation by Platinum(II) and Palladium(II) Complexes

	Temperature	m ($\text{kJ mol}^{-1})(\text{mM})^{-1}$)	$\Delta G^\circ_{(H_2O)}$ (kJ mol^{-1})	$\Delta H^\circ_{(H_2O)}$ (kJ mol^{-1})	$\Delta S^\circ_{(H_2O)}$ ($\text{kJ mol}^{-1} \text{K}$)
$[\text{Pt}(\text{bpy})(\text{Et-dtc})]\text{NO}_3$	27 °C	138.90	17.43	28.94	0.04
	37 °C	134.74	15.93		
$[\text{Pd}(\text{bpy})(\text{Et-dtc})]\text{NO}_3$	27 °C	159.03	18.81	48.90	0.10
	37 °C	158.4	17.81		

m = measure of the metal complex ability to denature DNA. $\Delta G^\circ_{(H_2O)}$ = conformational stability of DNA in the absence of metal complex. $\Delta H^\circ_{(H_2O)}$ = the heat needed for DNA denaturation in the absence of metal complex. $\Delta S^\circ_{(H_2O)}$ = the entropy of DNA denaturation by metal complex.

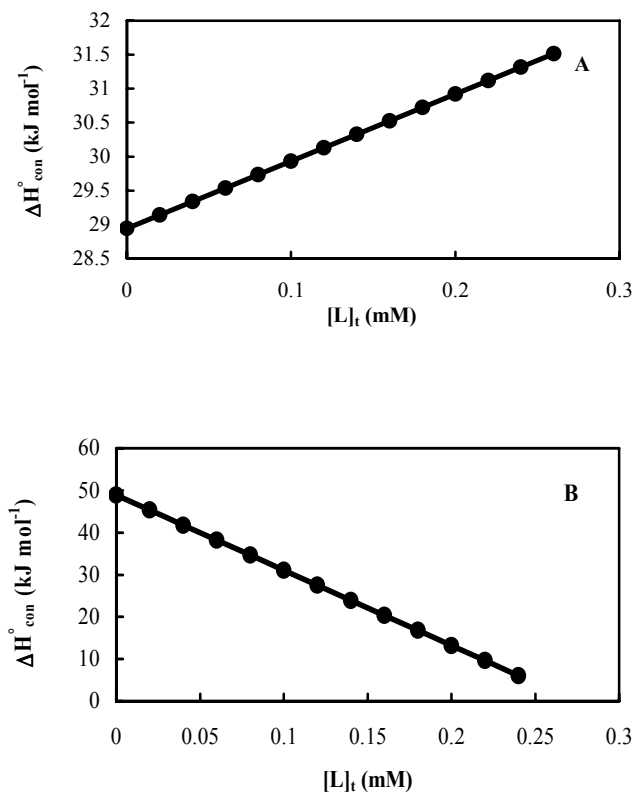


Fig. 9. The molar enthalpies of DNA denaturation in the interaction with (A) $[\text{Pt}(\text{bpy})(\text{Et-dtc})]\text{NO}_3$ and (B) $[\text{Pd}(\text{bpy})(\text{Et-dtc})]\text{NO}_3$ complexes in the range of 27°C to 37°C .

Another important thermodynamic parameter found is the molar enthalpy of DNA denaturation in the absence of metal complexes *i.e.* $\Delta H^{\circ}_{(H_2O)}$. For this, we calculated the molar enthalpy of DNA denaturation in the presence of each metal complex, $\Delta H^{\circ}_{\text{conformation}}$ or $\Delta H^{\circ}_{\text{denaturation}}$, in the range of the two temperatures using Gibbs-Helmholtz equation (Eq. (14)). On plotting the values of these enthalpies versus the concentrations of each metal complex, straight lines were obtained which are shown in Fig. 9(A) and 9(B) for $[\text{Pt}(\text{bpy})(\text{Et-dtc})]\text{NO}_3$ and $[\text{Pd}(\text{bpy})(\text{Et-dtc})]\text{NO}_3$, respectively. Intrappolation of these lines (intercept on ordinate *i.e.*, absence of metal complex) give the values of $\Delta H^{\circ}_{(H_2O)}$ (see Table 4). These plots show that in the range of 27°C to 37°C the

changes in the enthalpies in the presence of Pd(II) complex are descending while those of Pt(II) are ascending. These observations indicate that on increasing the concentration of Pd(II) complex, the stability of DNA is decreased while in the case of Pt(II) the opposite trend is observed, which may be due to higher tendency of interaction of Pd(II) rather than Pt(II) complexes with DNA.

In addition, the entropy ($\Delta S^{\circ}_{(H_2O)}$) of DNA unfolding by Pt(II) and Pd(II) complexes was calculated using Eq. (15). The related data are given in Table 4. These data show that the metal-DNA complex is more disordered than the native DNA, because the entropy changes are positive and the extent of disorder in Pd(II)-DNA complex is more than Pt(II)-DNA complex (see Table 4). This again shows that ability of Palladium complex in the denaturation of DNA is more than that of the Platinum complex.

In a further study, the solution of each interacting DNA-metal complex was passed through a Sephadex G-25 column equilibrated with the same buffer. Elution was done with buffer and each fraction of the column was monitored spectrophotometrically at 321 nm and 258 nm for Pt(II)-DNA system and 313 nm and 258 nm for Pd(II)-DNA system. The gel chromatograms obtained from these experiments are given in Figs. 10. These results show that the two peaks obtained at two wavelengths were not clearly resolved in Fig. 10(A), which indicates that metal complexes were not separated from DNA and their binding with DNA is strong enough not to break readily. This type of binding of metal complexes to DNA is strictly true for kinetically inert Platinum(II)-DNA complex. However, in the case of Palladium(II)-DNA system, two peaks were observed for both wavelengths and none of them were resolved in Fig. 10(B). This indicates that in the presence of Palladium(II) complex, DNA partially breaks into two fractions, one with higher and the second with lower molecular weight. Surprisingly, the amount of Palladium(II) metal complex bound to the fraction with lower molecular weight is higher than the amount bound to the fraction with higher molecular weight as is clear from the absorption readings at 313 nm. To confirm the breaking of DNA by this metal complex, a solution of the same DNA was passed through the same column and each eluted fraction of 2 ml was monitored at 258 nm. The gel chromatogram obtained is shown in Fig. 10(C). This indicates that the highly

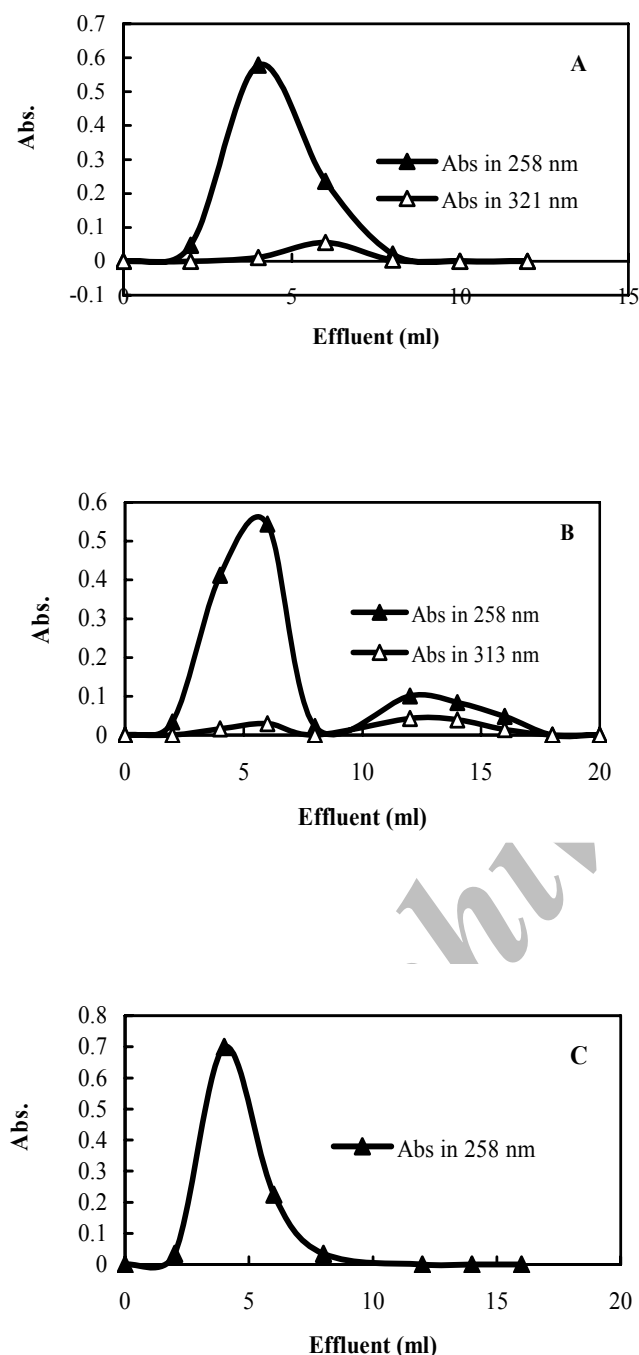


Fig. 10. Gel chromatograms of (A) $[Pt(bpy)(Et-dtc)]NO_3$ -DNA complex, (B) $[Pd(bpy)(Et-dtc)]NO_3$ -DNA complex and (C) only DNA, obtained on Sephadex G-25 column, equilibrated with 10 mM Tris-HCl buffer of pH 7.0 in the presence of 0.01 M sodium chloride.

polymerized calf thymus DNA has fractions with approximately similar molecular weights. The above results of Sephadex G-25 column compare well with those of $[M(bpy)(AA)]^+$, where M is Pt or Pd and AA is an anion of glycine or alanine complexes as reported earlier [49].

The interaction between metal complexes and DNA was further studied by changing the ionic strength of the medium [37]. Increasing the ionic strengths either by 100 mM NaCl or 0.6 mM $MgCl_2$, reversed the binding of Pt(II)- or Pd(II)-DNA systems completely. This dependence of binding on ionic strength suggests that the electrostatic interactions and/or hydrogen bonding may be at work in interaction of the above complexes with DNA.

The involvement of hydrogen bonding between DNA and metal complexes was also studied by precipitating the DNA from the interacted DNA-metal complexes with absolute ethanol. In this experiment the precipitated DNA was separated out and washed several times with ethanol. This precipitate was redissolved in Tris-HCl buffer and the solution was monitored spectrophotometrically for DNA at 258 nm, Pt(II) complex at 321 nm and Pd(II) complex at 313 nm. The presence of DNA-metal complex in this solution as observed by spectral method suggests that the involvement of hydrogen bond formation may be responsible for stabilizing the above DNA-metal complexes. Similar hydrogen bond formation was observed for $[Pt(bpy)(AA)]Cl$, where AA is an anion of amino acid [22].

The effect of the Pd(II) and Pt(II) complexes on the fluorescence spectrum of solutions containing the DNA and ethidium bromide has been investigated. It is known that the fluorescence intensity of ethidium bromide grows when it goes from a polar to a non-polar medium due to the lowering of the inter-system crossing lifetimes [38]. The displacement of DNA intercalated ethidium bromide by groove binding molecules has been used as a standard technique to assay DNA binding agents [39]. Ethidium bromide is a dye whose fluorescence is quenched in water, but strongly enhanced when it intercalates within DNA duplexes. The fluorescence emission spectra of the intercalated ethidium with increasing concentrations of Pd(II) and Pt(II) complexes are shown in Figs. 11. Figures 11 show a significant reduction of the ethidium emission intensity by adding different concentrations of Pd(II) and Pt(II) complex at different temperatures ($27^\circ C$

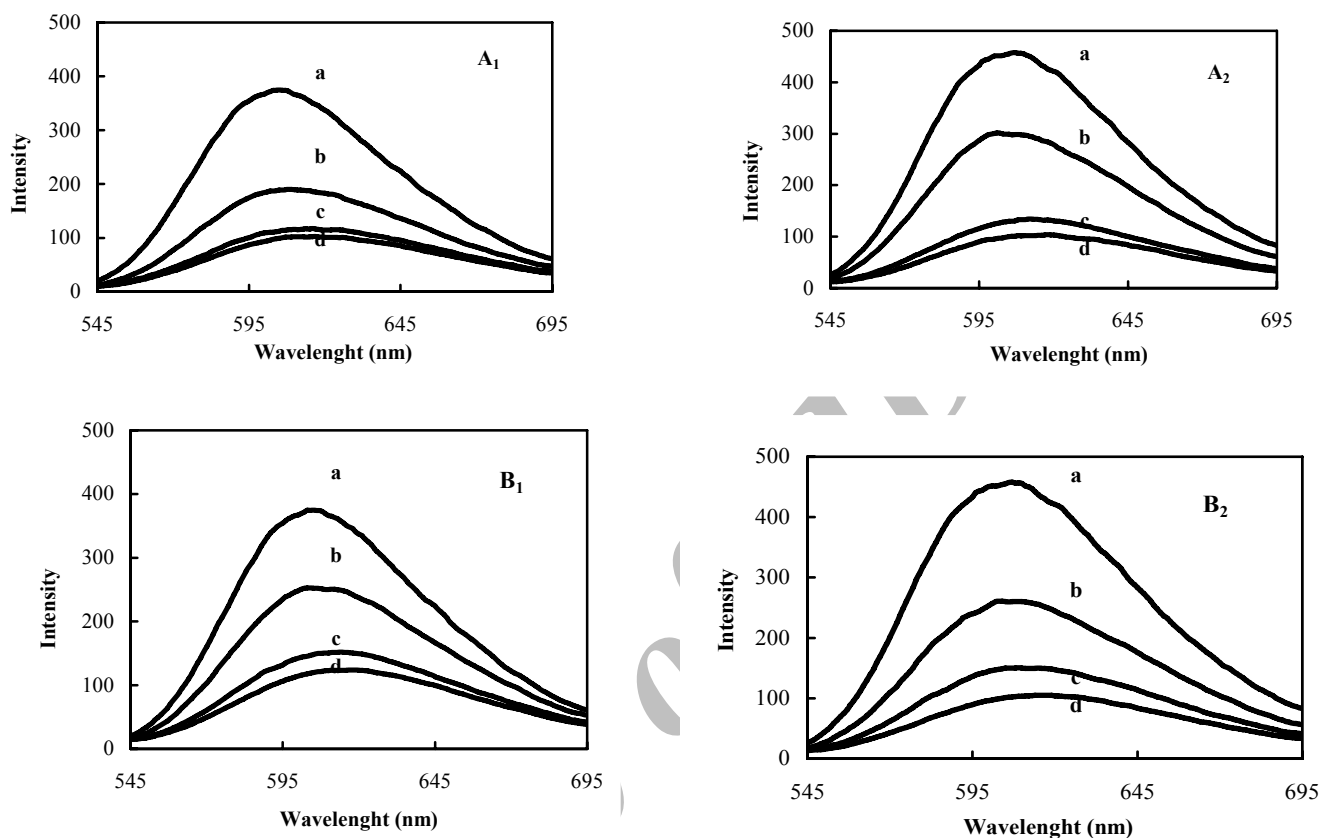


Fig. 11. Fluorescence emission spectra of interacted ethidium-DNA in the absence (a) and presence of different concentrations of Pt(II) complex (A_1 and A_2) and Pd(II) complex (B_1 and B_2): 0.05 mM (b); 0.1 mM (c); 0.15 mM (d) at 27 °C and 37 °C, respectively.

and 37 °C). It can be concluded that the fluorescence intensity of DNA intercalated ethidium is quenched when ethidium is removed from the duplexes by the action of Pd(II) and Pt(II) complexes and is released into water. These studies as well as the fluorescence Scatchard plots obtained for the reported analog, $[\text{Pd}(\text{bpy})(\text{ddtc})]\text{NO}_3 \cdot \text{H}_2\text{O}$, where ddtc is diethyldithiocarbamate [18] and the cooperative nature seen in the interaction studies using UV difference spectroscopic methods, allow us to conclude that our two complexes possibly intercalate in DNA through the planar 2,2'-bipyridine ligand present in their structures.

Circular dichroism (CD) spectroscopy was used to further examine the conformational aspects of the interaction of Pd(II) and Pt(II) complexes with DNA [38]. The observed CD spectrum of DNA consists of a positive band at 265 nm due to base stacking and a negative band at 247 nm due to helicity.

The complexes have no CD spectrum when free in the solution but have an induced CD spectrum when they interact with DNA. When our compounds were incubated with DNA, the CD spectra displayed changes of both positive and negative bands (Figs. 12). Moreover, at concentrations lower than $[\text{L}]_{1/2}$, the complexes may induce certain conformational changes in DNA as indicated by significant decrease in the intensities of positive and negative bands. However, at concentrations higher than $[\text{L}]_{1/2}$, the precipitate formed and spectra collapsed completely. Similar observations have been reported in the interaction of crocin and crocetin with calf thymus DNA [48].

CONCLUSIONS

Two water soluble Platinum(II) and Palladium(II)

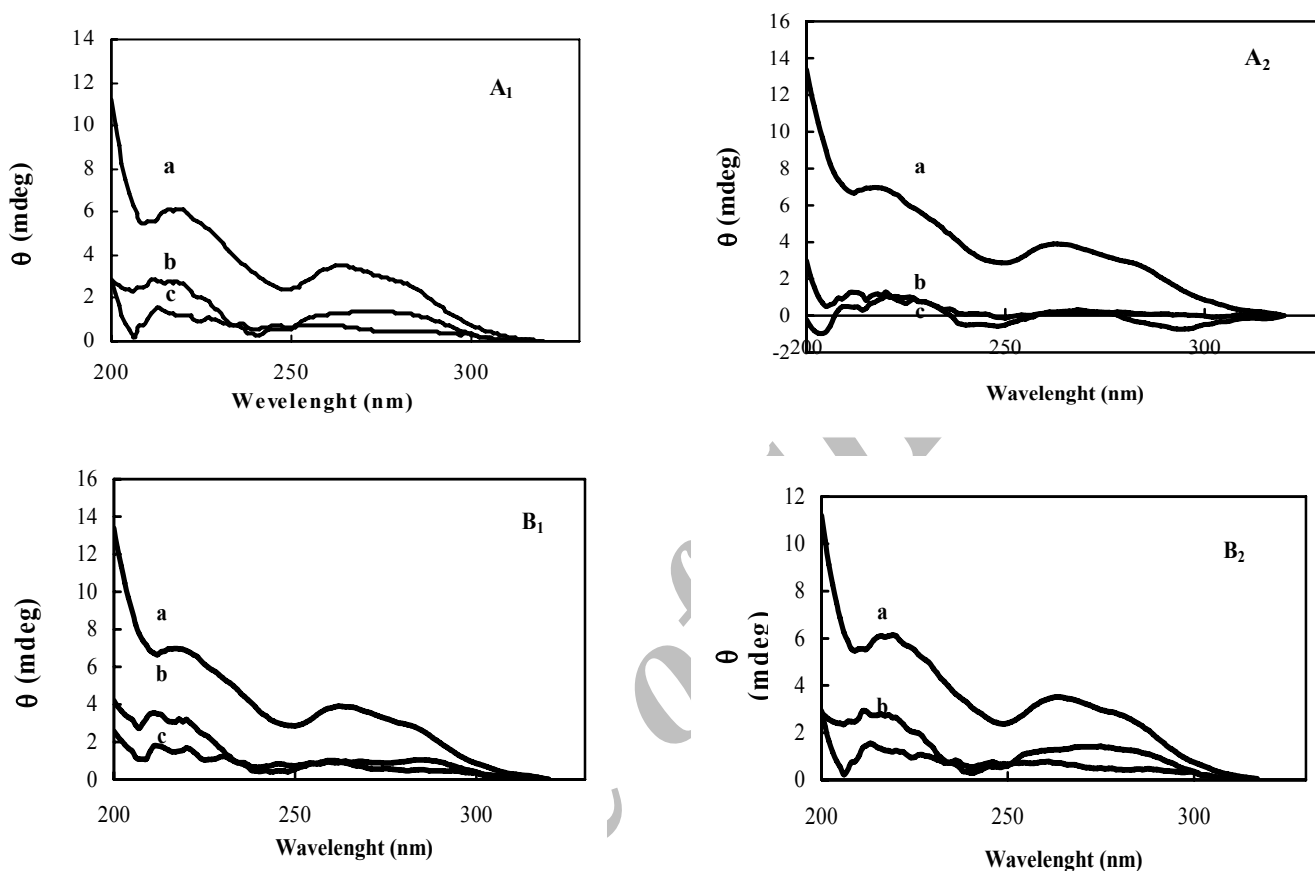


Fig. 12. CD spectra of DNA adduct with compound. plot for titration of DNA with the Pt(II) complex (A_1 and A_2) and Pd(II) complex (B_1 and B_2) at 27 °C and 37 °C, respectively. a: free DNA (120 μ M); b: in presence of 100 μ M complex and c: in the presence of 200 μ M complex.

complexes of bidentate nitrogen donors and bidentate sulfur donors chelating ligands were prepared and characterized. *In vitro* cytotoxic results suggested that the Pd(II) complex had more growth inhibitory activity against K562 relative to Pt(II) complex and both are more cytotoxic than cisplatin. Detailed interaction studies of both complexes with calf thymus DNA were carried out. They cooperatively bind to DNA and unexpectedly denature the DNA at very low concentrations. Other studies imply that the mode of binding of the complexes to DNA is possibly intercalation through the planar 2,2'-bipyridine ligand present in their structures and hydrogen binding may be operative in these interactions.

ACKNOWLEDGEMENTS

Financial assistance from the Research Council of the

University of Sistan and Bluchestan and the University of Tehran is gratefully acknowledged.

REFERENCES

- [1] B. Desoize, C. Madoulet, *Crit. Rev. Oncol./Hematol.* 42 (2002) 317.
- [2] L. Ronconi, L. Giovagnini, C. Marzano, F. Bettio, R. Ganziani, G. Pilloni, D. Fregona. *Inorg. Chem.* 44 (2005) 1867.
- [3] F. Shaheen, A. Badshad, M. Gielen, M. Dusek, K. Fejfarova, D. de Vos, B. Mirza, *J. Organomet. Chem.* 692 (2007) 3019.
- [4] A. Divsalar, A.A. Saboury, H. Mansouri-Torshizi, A.A. Moosavi-Movahedi, *J. Biomol. Struct. Dyn.* 25 (2007) 173.

- [5] Z. Guo, P.J. Sadler, *Adv. Inorg. Chem.* 49 (2000) 183.
- [6] A. Divsalar, A.A. Saboury, R. Yousefi, A.A. Moosavi-Movahedi, H. Mansouri-Torshizi, *Int. J. Biol. Macro.* 40 (2007) 381.
- [7] H. Mansouri-Torshizi, S. Ghadimy, N. Akbarzadeh, *Chem. Pharm. Bull.* 49 (2001) 1517.
- [8] H. Mansouri-Torshizi, M. Islami-Moghaddam, A.A. Saboury, *Acta Biochimica et Biophysica Sinica.* 35 (2003) 886.
- [9] M.P. Hacker, E.B. Douple, I.H. Krakoff. *Platinum Coordination Complexes in Cancer Chemotherapy*, Boston, M.A: Nijhoff Publisher, 1984, p. 267.
- [10] G. Hogarth, *Prog. Inorg. Chem.* 53 (2005) 71.
- [11] N. Manav, A.K. Mishra, N.K. Kaushik, *Spectrochim. Acta* 65 (2006) 32.
- [12] L. Ronconi, C. Maccato, D. Barreca, R. Saini, M. Zancato, D. Fregona, *Polyhedron.* 24 (2005) 521.
- [13] P.K. Somers, R.M. Modford, U. Saxena, *Free Radic. Biol. Med.* 28 (2000) 1532.
- [14] K.S. Siddiqi, S.A.A. Nami, L.U. Chebude, *J. Braz. Chem. Soc.* 17 (2006) 107.
- [15] L. Messori, F. Abbate, G. Marcon, P. Orioli, M. Fontani, E. Mini, T. Mazzei, S. Garotti, T.O. Conell, P. Zanello, *J. Med. Chem.* 43 (2000) 3541.
- [16] G. Marcon, S. Carotti, M. Coronello, L. Messori, E. Mini, P. Orioli, T. Mazzei, M.A. Cinellu, G. Minghetti, *J. Med. Chem.* 45 (2002) 1672.
- [17] K. Lemma, S.K.C. Elmroth, L.I. Elding, *J. Chem. Soc. Dalton trans* (2002) 1281.
- [18] R. Mital, N. Jain, T.S. Srivastava, *Inorg. Chim. Acta* 166 (1989) 135.
- [19] C. Marzano, D. Fregona, F. Baccichetti, A. Trevisan, L. Giovagnini, F. Bordin, *Chem. Biol. Interact.* 140 (2002) 215.
- [20] C. Marzano, A. Trevisan, L. Giovagnini, D. Fregona, *Toxicol. In Vitro.* 16 (2002) 413.
- [21] N. Farrell, *Met. Ions. Biol. Syst.* 32 (1996) 603.
- [22] R. Mital, K.S. Ray, T.S. Srivastava, R.K. Bahattacharya, *J. Inorg. Biochem.* 27 (1986) 133.
- [23] F.A. Palocsay, J.V. Rund, *Inorg. Chem.* 8 (1969) 524.
- [24] C.C. Hadjikostas, G.A. Katsoulos, M.P. Sigalas, C.A. Tsipis, *Can. J. Chem.* 67 (1989) 902.
- [25] R. Mital, T.S. Srivastava, *J. Inorg. Chem.* 40 (1990) 111.
- [26] A.M.Q. King, B.H. Nicholson, *Biochem. J.* 114 (1969) 679.
- [27] A.M.Q. King, B.H. Nicholson, *Ann. N.Y. Acad. Sci.* 51 (1949) 660.
- [28] A.A. Saboury, *J. Iran. Chem. Soc.* 3 (2006) 1.
- [29] A.V. Hill, *J. Physil (Lond.)* 40 (1910) 4.
- [30] A.A. Saboury, A.K. Bordbar, A.A. Moosavi-Movahedi, *Bull. Chem. Soc. Jp.* 69 (1996) 3031.
- [31] M.L. James, G.M. Smith, J.C. Wolford, *Applied Neumerical Methods for Digital Computer*, 3rd ed., New York, USA, Harper and Row Publisher, 1985.
- [32] A.A. Saboury, A.A. Moosavi-Movahedi, H. Mansouri-Torshizi, *J. Chin. Chem. Soc.* 46 (1999) 917.
- [33] G.M. Barrow. *Physical Chemistry*, chap. 7, 5th ed., MC Graw-Hill, New York, 1988.
- [34] R.F. Greene, C.N. Pace, *J. Biol. Chem.* 249 (1974) 5388.
- [35] M. Ghadermarzi, A.A. Saboury, A.A. Moosavi-Movahedi, *Polish J. Chem.* 72 (1998) 2024.
- [36] P.W. Atkins, *Physical Chemistry*, Chap. 5, 6th ed., Oxford University Press, Oxford, 1998.
- [37] H. Mansouri-Torshizi, T.S. Srivastava, S.J. Chavan, M.P. Chitnis, *J. Inorg. Biochem.* 48 (1992) 63.
- [38] A.G. Krishna, D.V. Kumar, B.M. Khan, S.K. Rawal, K.N. Ganesh, *Biochim. Biophys. Acta* 1381 (1998) 104.
- [39] L. Peres-Flores, A.J. Ruiz-Chica, J.G. Delcros, F.M. Sanches, F.J. Ramirez, *Spectrochim. Acta Part A* 69 (2008) 1089.
- [40] R.J. Angelici, *Synthesis Technique in Inorganic Chemistry*, Saunders, Philadelphia, 1969, pp.17.
- [41] N. Jain, T.S. Srivastava, *Inorg. Chim. Acta* 128 (1987) 151.
- [42] D. Coucouvanis, in: S.J. Lippard (Ed.), *Progress in Inorganic Chemistry*, Vol. 11, Willey, New York, 1970, pp. 311.
- [43] G.P. Katsoulos, G.F. Mannoussakis, C.A. Tsipis, *Polyhedron.* 3 (1984) 735.
- [44] A. Manohar, K. Ramalingam, G. Bocelli, L. Righi, *Inorg. Chim. Acta* 314 (2001) 177.
- [45] V. Alverdi, L. Giovagnini, C. Marzano, R. Seraglia, F. Bettio, S. Sitran, R. Graziani, D. Fregona, *J. Inorg. Biochem.* 98 (2004) 1117.

- [46] L. Kumar, N.R. Kandasamy, T.S. Srivastava, A.J. Amonkar, M.K. Adwankar, M.P. Chitnis, *J. Inorg. Biochem.* 23 (1985) 1.
- [47] Z.H. Xu, F.J. Chen, P.X. Xi, X.H. Liu, Z.Z. Zeng, *J. Photochem. Photobiol A: Chem.* 196 (2008) 77.
- [48] S.Z. Bathaie, A. Bolhasani, R. Hoshyar, B. Ranjbar, F. Sabouni, A.A. Moosavi-Movahedi, *DNA and Cell Biol.* 26 (2007) 533.
- [49] A.K. Paul, H. Mansouri-Torshizi, T.S. Srivastava, *J. Inorg. Biochem.* 50 (1993) 9.

Archive of SID